An Ultraluminous X-Ray Object with a 2 Hour Period in M51

Ji-Feng Liu – University of Michigan
Joel N. Bregman – University of Michigan
Jimmy Irwin – University of Michigan
Patrick Seitzer – University of Michigan

Citation of published version:

Liu, J., Bregman, J., Irwin, J., Seitzer, P. (2002): An Ultraluminous X-Ray Object with a 2 Hour Period in M51. *The Astrophysical Journal Letters*, 581(2). DOI: 10.1086/346101

THE ASTROPHYSICAL JOURNAL, 581:L93–L96, 2002 December 20

AN ULTRALUMINOUS X-RAY OBJECT WITH A 2 HOUR PERIOD IN M51

JI-FENG LIU, JOEL N. BREGMAN, JIMMY IRWIN, AND PATRICK SEITZER
Astronomy Department, University of Michigan, MI 48109
Received 2002 October 22; accepted 2002 November 13; published 2002 November 27

ABSTRACT

Ultraluminous X-ray objects (ULXs) are off-nucleus point sources with $L_X = 10^{39}$–10^{41} ergs s^{-1}, but the nature of such systems is largely unidentified. Here we report a 2.1 hr period observed in a *Chandra* ACIS observation for ULX M51 X-7, which is located on the edge of a young star cluster in the star-forming region in a spiral arm. In two ACIS observations separated by 1 yr, the ULX changed from a high-hard to a low-soft spectral state, in contrast to most Galactic low-mass X-ray binaries. On the basis of its period and spectral behaviors, we suggest that this ULX is a low-mass X-ray binary system, with a dwarf companion of 0.2–0.3 $M_\odot$ and a compact accretor, either a neutron star or a black hole, whose mass is not well constrained. Relativistic beaming effects are likely involved to produce the observed high X-ray luminosities, given its low accretion rate as inferred from a sustainable accretion scenario via Roche lobe overflow.

Subject headings: galaxies: individual (M51) — X-rays: binaries

1. INTRODUCTION

X-ray emission from active galactic nuclei and quasars, powered by accretion onto nuclear supermassive black holes, is usually greater than 10^{41} ergs s^{-1}, while for the stellar binary systems in the Milky Way, the luminosities are typically 10^{33}–10^{38} ergs s^{-1}. X-ray objects with luminosities of 10^{39}–10^{41} ergs s^{-1} have been observed in some external galaxies as off-nucleus point sources by X-ray satellites such as *Einstein*, *ROSAT*, *ASCA*, and recently the *Chandra X-Ray Observatory* (e.g., Fabbiano 1989; Marston, Elmegreen, & Elmegreen 1995; Zezas et al. 2002). These objects have several names, a popular designation being "ultraluminous X-ray objects" or ULXs.

One suggestion for the nature of these ULXs is that they are binary systems with 10^3–10^4 $M_\odot$ black holes as primaries (Colbert & Mushotzky 1999). Such black holes, if they exist, are the missing links between stellar-mass black holes and supermassive black holes in the nuclei of galaxies. This suggestion is consistent with the X-ray spectra of some ULXs (Makishima et al. 2000). However, the formation of such massive black holes is not predicted by stellar evolution theory, and it may be impossible to form such objects even in dense star clusters. Alternatively, these sources may be stellar-mass black holes or neutron stars whose emission is beamed, thereby representing microquasars (King et al. 2001; King 2002). If the emission is beamed, the intrinsic luminosities become sub-Eddington, and there are known examples of beamed Galactic X-ray sources (cf. Mirabel & Rodriguez 1999). It is also possible that the luminosities are truly super-Eddington, for example, obtainable from accretion disks with radiation-driven inhomogeneities (Begelman 2002).

To identify which of the above suggestions is correct, one natural and fruitful way is to associate them with known classes of objects by comparing spectral behaviors, short-term and long-term variabilities, etc. Spectral analyses of ULXs, not without problems, generally support the mass-accreting black hole scenarios (e.g., Makishima et al. 2000). Spectral transitions were observed for two ULXs in IC 342 between high-soft and low-hard states, reminiscent of some black hole X-ray binaries in our Galaxy (Kubota et al. 2001). While many ULXs are variable during individual observations, few periods have been reported. So far, a 7.5 hr period has been found for a ULX in the Circinus galaxy (Bauer et al. 2001; Bianchi et al. 2002), and a possible periodicity at several tens of hours of a ULX in IC 342 has been reported (Sugiho et al. 2001). In this Letter, we report a 2.1 hr period for a ULX in M51 (NGC 5194), M51 X-7, as designated in Roberts & Warwick (2000). This ULX is located on the outskirts of a young open cluster on a spiral arm of M51. In § 2, we present the two *Chandra* ACIS observations utilized and the results. A period of 7620 s for the ULX is found from the X-ray light, and a spectral transition is found between two *Chandra* observations. In § 3, we discuss the implications of its period and spectral evolution and suggest that this ULX is a low-mass X-ray binary system, with a dwarf companion of 0.2–0.3 $M_\odot$ and a compact accretor. Possible mechanisms to produce the high X-ray luminosity are also discussed. For the distance to M51, we use 7.7 Mpc (Roberts & Warwick 2000).

2. DATA ANALYSIS AND RESULTS

Two *Chandra* ACIS observations of M51, observation ID (ObsID) 354 (15 ks, 2000 June 20) and ObsID 1622 (27 ks, 2001 June 23), were retrieved from the archive. The data were analyzed with CIAO 2.2.1, CALDB 2.12, XSPEC 11.2.0, and XRONOS 5.19. Pixel randomization of event positions was removed to recover the original positions before CIAO task WAVDETECT was used to detect discrete sources on ACIS-S chips. The accuracy of absolute positions for these sources is expected to be 0.″6 (Aldcroft et al. 2000).

The ULX M51 X-7 was observed in both data sets, with ACIS positions differing by (0.″5, 0.″1). For the true position, we take the average, i.e., R.A. = $13^h30^m0\overset{s}{.}99$, decl. = 47°13′43.″9, with a positional uncertainty of 0.″4. Registering this position onto a *Hubble Space Telescope* (*HST*) Wide Field Planetary Camera 2 (WFPC2) image, we find that it falls onto the edge of a star cluster in a dusty star-forming knot on a spiral arm of M51. Within its positional error circle are a few stars fainter than 23 mag. The details of its potential optical counterpart will be reported in a future paper.

For timing and spectral analyses, we selected circular apertures with such sizes that the number of source photons outside the aperture is approximately the number of background photons inside the aperture. The size chosen is 4.″0 for ObsID 354 and 2.″0 for ObsID 1622. The light curve of X-7 in the first ACIS observation (ObsID 354), defined by about 550 photons, appears

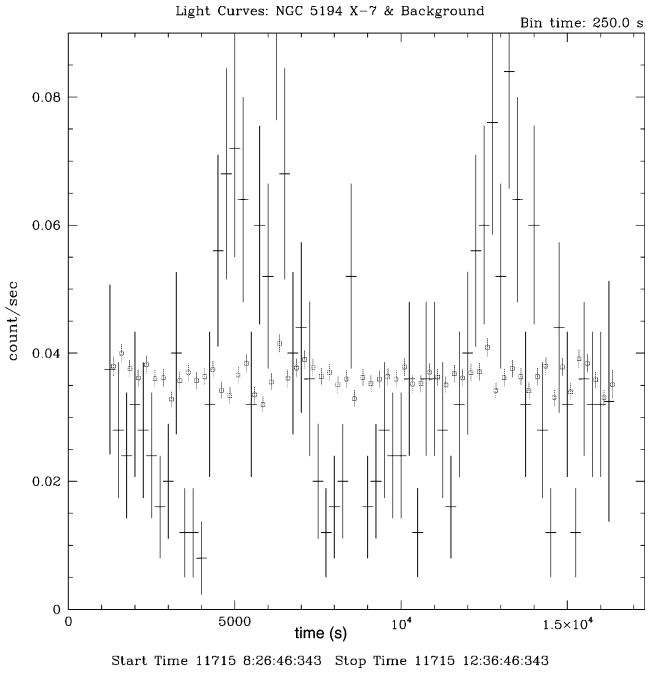

FIG. 1.—Light curve of M51 X-7 in ACIS observation ObsID 354. The ULX flux varies periodically by an amplitude of more than 50%. The overlaid light curve labeled by squares is the scaled background, which shows variation of less than 10%. Photons within 0.3–10 keV were used for the light curves.

to have the structure of a single period, as shown in Figure 1 in contrast with the background light curve. When fitting a periodic signal, we derive a period of 7620 s (using XRONOS/efsearch with 10 s resolution). The uncertainty in the period is approximately 500 s (a more accurate value is not possible because of the limited number of periods involved). To determine whether this could be an instrumental effect, we carried out a number of tests. We formed the light curves of all other bright sources in the same ACIS field but found no evidence for periods. The period cannot be caused by background variation, since the count rate of the background varies by less than 10% (and is not periodic), while the count rate of X-7 varies by an amplitude of more than 50%, for both soft photons (<1.5 keV) and hard photons (>1.5 keV).

Dithering may cause spurious periods when a source is dithering across a CCD node boundary or gap, falls off the detector, or crosses bad pixels periodically. In this observation, the dither period is 1000 s in the chip *Y* direction and 700 s in the chip *X* direction. The dither pattern is a Lissajous figure, spanning 16″ from peak to peak. The ULX falls on node 2 of chip S3 at (556, 459). It is 22″ away from the node 1–2 boundary, and no bad pixels fall within 30″ of the source. Thus, it is unlikely that the period is due to the dithering period.

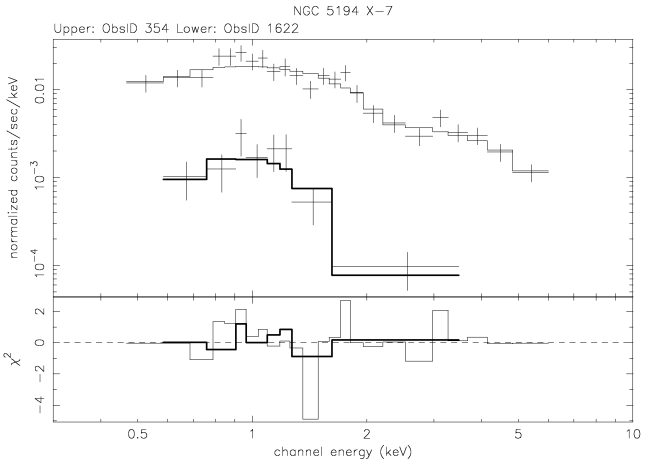

FIG. 2.—Spectral fits of M51 X-7 in two ACIS observations. In the first observation (ObsID 354), the ULX was in a high-hard state, while in the second observation (ObsID 1622, model and χ^2 in thick lines), it changed to a low-soft state.

In the second ACIS observation (ObsID 1622) that was taken 1 yr after the first, only 53 photons were collected for the ULX, too few to make a reliable periodicity analysis. Note that the second observation was longer than the first by a factor of about 1.8, so the photon flux in the 0.3–10 keV decreased by a factor of about 18 between these two observations.

Photons in the 0.3–8 keV band are used to perform spectral fits for both spectra, as shown in Figure 2. The CIAO thread ACISSPEC was used to extract the spectra, and CORRARF was used to correct the continuous degradation in the ACIS quantum efficiency. To get good χ^2 statistics, we grouped the first spectrum (ObsID 354) requiring a minimum of 20 photons per bin. For the second spectrum (ObsID 1622), we required a minimum of 5 photons per bin to get enough bins. We tried absorbed (wabs) power-law (powerlaw), absorbed multicolor disk (diskbb), and absorbed blackbody (bb) models on each spectrum. In Table 1, we list the best-fit parameters; the errors for the best-fit parameters are for the 90% confidence level. For the first spectrum, an absorbed blackbody model is not acceptable, but an absorbed power-law model is acceptable, with a power-law photon index $\Gamma = 1.25^{+0.24}_{-0.22}$, and an absorbed multicolor disk model is also acceptable, with an inner edge temperature $kT_{\rm in} = 2.10^{+0.63}_{-0.40}$ keV. To test whether there is an additional component due to a neutron star solid surface, we also fit an absorbed (multicolor disk + 2 keV blackbody) model to the first spectrum. With one more free parameter, this model improves the spectral fit marginally, as compared to an absorbed multicolor disk model, and results in a smaller inner edge temperature, $kT_{\rm in} = 0.82^{+1.57}_{-0.30}$ keV. However, this addi-

TABLE 1
SPECTRAL FITS FOR M51 X-7 IN TWO ACIS OBSERVATIONS

ObsID	Model	$N_{\rm H}$ ($\times 10^{22}$ cm^{-2})	Γ	$kT_{\rm in}$ (keV)	kT	χ^2_ν/dof	Absorbed $L_{\rm X}$[a] ($\times 10^{38}$ ergs s^{-1})	Unabsorbed $L_{\rm X}$[a] ($\times 10^{38}$ ergs s^{-1})
354	wabs*powerlaw	$0.06^{+0.07}_{-0.06}$	$1.25^{+0.24}_{-0.22}$	...	...	0.95/21	18.6	19.8
	wabs*diskbb	<0.03	...	$2.12^{+0.71}_{-0.42}$	...	1.06/21	17.1	17.1
	wabs*bb	...	...	...	...	3.47/21	...	...
	wabs*(bb+diskbb)	$0.02^{+0.09}_{-0.02}$	...	$0.82^{+1.57}_{-0.30}$	2.0 (frozen)	1.01/20	18.8	19.2
1622	wabs*powerlaw	$0.70^{+1.02}_{-0.55}$	>2.6	...	...	0.82/5	0.39	9.34
	wabs*diskbb	$0.27^{+1.09}_{-0.27}$	...	0.29 ± 0.09	...	0.89/5	0.30	0.77
	wabs*bb	...	...	...	...	4.61/7	...	...

[a] The X-ray luminosities are for 0.3–8 keV.

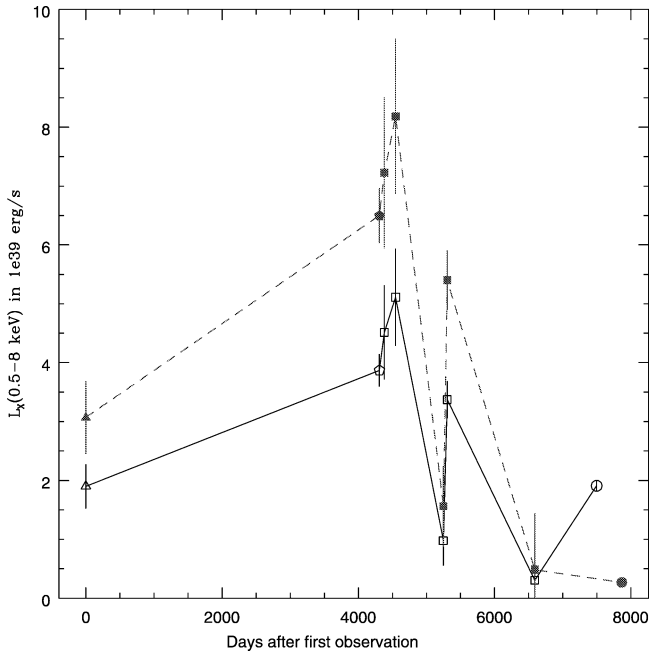

FIG. 3.—Long-term variability of M51 X-7. Extracted from the archive were one *Einstein* HRI observation (*triangles*), one *ROSAT* Position Sensitive Proportional Counter (PSPC) observation (*pentagons*), five *ROSAT* HRI observations (*squares*), and two *Chandra* ACIS observations (*circles*). The instrumental count rates were converted to flux assuming absorbed power-law models (1) if in the high-hard state (*open symbols*) and (2) if in the low-soft state (*filled symbols*). A distance of 7.7 Mpc was assumed to convert fluxes to luminosities.

tional component does not make a better model than a simple absorbed power-law model.

For the second spectrum, an absorbed power-law model gives a power-law photon index of $\Gamma > 2.6$, an absorbed multicolor disk model gives an inner edge temperature of $kT_{\rm in} = 0.29 \pm 0.09$ keV, while an absorbed blackbody model is not acceptable. As compared with the first spectrum of higher photon flux, the second spectrum is much softer, and the best-fit absorbing column density is higher, too. For simple absorbed power-law models, we switched the photon indices of the two spectra and fitted a frozen $\Gamma = 2.6$ to the first spectrum and a frozen $\Gamma = 1.25$ to the second spectrum, and we found that both models can be accepted only on the levels less than 10^{-2}. Thus, we conclude that the first spectrum is truly harder than the second spectrum. Absorbed power-law models with smaller frozen $n_{\rm H}$ values were also fitted to the second spectrum and gave worse fits, indicating that the high column density in the second spectrum is real.

3. DISCUSSION

Periods are not uncommon in Galactic X-ray point sources, such as cataclysmic variables (CVs), low-mass X-ray binaries (LMXBs), and high-mass X-ray binaries (HMXBs). HMXBs have periods of more than a few days, because they are usually widely separated systems. A 2 hr period is common for CVs, in which the accretor and the donor are white dwarfs. However, CV systems have typical temperatures under 10^6 K, with most of the radiation emitted in the ultraviolet region and with X-ray luminosities below 10^{34} ergs s^{-1}. LMXBs usually have periods of 10+ hr, but they can have periods as short as 1 hr, for example, 1624−490 has a period of 0.69 hr. The source studied here, with a period of 2 hr and a temperature of ~1 keV, is most similar to the LMXBs.

The LMXB picture of ULXs does not contradict its location in a star-forming region. While observations show that ULXs preferentially occur in active star-forming regions (e.g., Zezas et al. 2002), indicating their short lifetimes, they nevertheless could be a short stage in the long lifetime of LMXBs. Indeed, some ULXs have also been found outside star-forming regions, for example, in gas-poor elliptical galaxies such as NGC 1399 (Angelini, Loewenstein, & Mushotzky 2001) and in a globular cluster on the outskirt of the bulge in edge-on spiral galaxy NGC 4565 (Wu et al. 2002).

If X-7 is an LMXB with an orbital period of about 2 hr, there are a number of implications. The secondary star would be filling its Roche lobe and undergoing mass loss to the primary, and from this picture, we can estimate the mass of the secondary, M_1. For a mass ratio of $q = M_1/M_2 < 0.8$, the Roche lobe radius is $R_{\rm cr} = 0.46a\,[M_1/(M_1 + M_2)]^{1/3}$ (Paczyński 1967), in which a is the separation between the donor and the accretor and M_2 is the mass of the accretor. Combined with Kepler's third law, this leads to $P_{\rm orb} = 8.9(R_1/R_\odot)^{3/2}(M_\odot/M_1)^{1/2}$ hr. For a late-type low-mass star, if we adopt an analytical mass-radius relation $R_1/R_\odot = M_1/M_\odot$ (Verbunt 1993), we obtain the mass of the donor to be $M_1 \approx 0.23\ M_\odot$. We also tried to obtain the mass of the donor by adopting a computed mass-radius relation from the Geneva stellar models (Lejeune & Schaerer 2001). We extended the star mass down to $0.1\ M_\odot$ by extrapolating computed $\log R$– $\log M$ relation for low-mass stars ($0.8 < M/M_\odot < 0.9$). These computed stellar models give an equivalent analytical relation of $R_1/R_\odot \approx (M_1/M_\odot)^{1.2}$, and the resulted donor mass is about $0.3\ M_\odot$. Such a low-mass secondary in M51 is impossible to identify, even with the *HST*.

The mass of the accretor cannot be constrained by the period under our assumptions. The accretor is most likely a neutron star or a black hole, as a compact object is needed to produce the observed hard spectra. One can refine this suggestion further by comparing the observed spectrum with models of compact objects, as we try here. Neutron star LMXBs and black hole LMXBs at high luminosities might be distinguished by their spectral features (cf. Tanaka & Lewin 1995), since high-luminosity neutron star LMXBs exhibit a multicolor disk component and a blackbody component with a color temperature of ~2 keV, which is interpreted as emission from the neutron star surface, while black hole LMXBs do not show such a single-color blackbody component at any luminosity level. As the luminosity decreases further, the spectrum becomes a single power law and distinction between black hole and neutron star LMXBs diminishes. For X-7, the model with an additional 2 keV thermal component improves the spectral fit marginally as compared to an absorbed multicolor disk model, which may be very weak evidence that the accretor is a neutron star. However, such a marginal improvement may be due to the additional freedom of parameters and does not really reflect the preference of a thermal component. Also, its trend of spectral transition from a hard-high state to a soft-low one has some Galactic parallels, such as Nova Muscae 1991 (Ebisawa et al. 1994), whose system is composed of a low-mass companion and a black hole of $\sim 6\ M_\odot$. Such spectral transitions, as noted by Terashima & Wilson (2002), are in contradiction to most Galactic LMXBs, which switch between soft-high and hard-low states. Thus, it is premature to identify it as a neutron star or a black hole with current observations.

One concern about this picture is that mass transfer from the less massive donor to the accretor will widen the orbit and enlarge

the Roche lobe with respect to the donor and thus prevent further mass transfer via Roche lobe overflow. This can be avoided if the orbit angular momentum can be dissipated effectively by gravitational radiation, with the rate $-(\dot{J}/J)_{\rm GR} = (32G^3/5c^5) \times M_1M_2(M_1 + M_2)/a^4$. The separation a evolves according to the equation $\dot{a}/a = 2\dot{J}/J - 2(1 - M_1/M_2)\dot{M}_1/M_1$ under conservative mass transfer via Roche lobe overflow (Verbunt 1993). In order for the orbit not to widen, the mass transfer rate via Roche lobe overflow must be less than a value of about 10^{-9} to 10^{-8} $M_\odot$ yr^{-1} for a primary of 3–100 $M_\odot$. In a steady state, accretion disks with these accretion rates generate luminosities of 10^{37}–10^{38} ergs s^{-1}, regardless of the mass of the accretor, less than the 10^{39} ergs s^{-1} we observed for X-7. The larger observed energy would require an additional phenomenon, such as a transient outburst or relativistic beaming. For example, X-ray novae can have substantial outbursts but usually with a duty cycle of less than 10%. However, this source has been brighter than 10^{39} ergs s^{-1} during the past two decades (Fig. 3), in conflict with expectations for dwarf novae. Therefore, the more likely explanation for the high luminosities is by relativistic beaming, as suggested by King et al. (2001).

An alternative model for the binary and the periodicity is that the period arises because of a hot spot in the accretion disk around the primary. This picture removes the restrictions on the mass of the secondary and its separation from the primary. If we assume Keplerian motion of the hot spot around the accretor, this 2 hr period corresponds to a distance of ~1–2 $R_\odot$ for an accretor mass of ~3–10 $M_\odot$. At such distances, the multicolor disk temperature is normally 10^4 K. A hot spot at such distances fails to explain the fluctuation amplitude for hard photons (>1.5 keV).

Another possibility is that the period is not real and results from the limited sampling of a randomly variable object. If the period reflects that of orbital motion, it should be highly reproducible, provided that the source is sufficiently bright. If it is due to the motion of a hot spot on a disk, one might expect the hot spot to fade with time (then the period would vanish while the source might still be luminous) or the spot might move inward in the disk, leading to a shorter period. Additional observations that could distinguish between these expectations would be greatly beneficial in clarifying the nature of the variation seen in M51 X-7.

We are grateful for the service of the *Chandra* Data Archive. We would like to thank Renato Dupke, Eric Miller, Franz Bauer, Rick Rothschild, and Steven Murray for helpful discussions. We gratefully acknowledge support for this work from NASA under grants HST-GO-09073.

REFERENCES

Aldcroft, T. L., et al. 2000, Proc. SPIE, 4012, 650
Angelini, L., Loewenstein, M., & Mushotzky, R. F. 2001, ApJ, 557, L35
Bauer, F. E., Brandt, W. N., Sambruna, R. M., Chartas, G., Garmire, G. P., Kaspi, S., & Netzer, H. 2001, AJ, 122, 182
Begelman, M. C. 2002, ApJ, 568, L97
Bianchi, S., Matt, G., Fiore, F., Fabian, A. C., Iwasawa, K., & Nicastro, F. 2002, A&A, in press (astro-ph/0209583)
Colbert, E. J. M., & Mushotzky, R. F. 1999, ApJ, 519, 89
Ebisawa, K., et al. 1994, PASJ, 46, 375
Fabbiano, G. 1989, ARA&A, 27, 87
King, A. R. 2002, MNRAS, 335, L13
King, A. R., Davies, M. B., Ward, M. J., Fabbiano, G., & Elvis, M. 2001, ApJ, 552, L109
Kubota, A., et al. 2001, ApJ, 547, L119
Lejeune, T., & Schaerer, D., 2001, A&A, 366, 538
Makishima, K., et al. 2000, ApJ, 535, 632
Marston, A. P., Elmegreen, D., & Elmegreen, B. 1995, ApJ, 438, 663
Mirabel, I. F., & Rodriguez, L. F. 1999, ARA&A, 37, 409
Paczyński, B. 1967, Acta Astron., 17, 287
Roberts, T. P., & Warwick, R. S. 2000, MNRAS, 315, 98
Sugiho, M., Kotoku, J., Makishima, K., Kubota, A., Mizuno, T., Fukazawa, Y., & Tashiro, M. 2001, ApJ, 561, L73
Tanaka, Y., & Lewin, W. H. G. 1995, in X-Ray Binaries, ed. W. H. G. Lewin, J. van Paradijs, & E. P. J. van den Heuvel (Cambridge: Cambridge Univ. Press), 265
Terashima, Y., & Wilson, A. 2002, in Proc. New Visions of the Universe in the *XMM-Newton* and *Chandra* Era, in press (astro-ph/0204321)
Verbunt, F. 1993, ARA&A, 31, 93
Wu, H., Xue, S. J., Xia, X. Y., Deng, Z. G., & Mao, S. D. 2002, ApJ, 576, 738
Zezas, A., Fabbiano, G., Rots, A. H., & Murray, S. S. 2002, ApJ, 577, 710